IEEE Access
Multidisciplinary ⋮ Rapid Review ⋮ Open Access Journal

Received 10 June 2024, accepted 21 June 2024, date of publication 3 July 2024, date of current version 12 July 2024.

Digital Object Identifier 10.1109/ACCESS.2024.3422398

RESEARCH ARTICLE

Identification of Maritime Areas With High Vessel Traffic Based on Polygon Shape Similarity

HAK-CHAN KIM[1], WOO-JU SON[2], JEONG-SEOK LEE[3], AND IK-SOON CHO[4]

[1]Graduate School, National Korea Maritime & Ocean University, Busan 49112, South Korea
[2]Department of Maritime AI and Cyber Security, National Korea Maritime & Ocean University, Busan 49112, South Korea
[3]Maritime Big Data and AI Center, Korea Institute of Ocean Science and Technology, Busan 49112, South Korea
[4]Division of Maritime AI and Cyber Security, National Korea Maritime & Ocean University, Busan 49112, South Korea

Corresponding author: Ik-Soon Cho (ischo@kmou.ac.kr)

This work was supported by the Development of Simulation Technology for Maritime Spatial Policy by the Ministry of Oceans and Fisheries under Grant 20220431.

ABSTRACT As new forms of industries emerge in marine spaces due to global environmental protection trends and the promotion of recreational activities, traditional navigation areas for vessels are also being affected. To ensure safe vessel passage and effective vessel traffic management in response to evolving maritime environments, navigational routes for ships must be exclusively established. Numerous studies have attempted to derive shipping routes from historical vessel-traffic data; however, the final forms of polygon shapes representing routes have not been produced. Hence, this study aimed to extract polygonal routes based on densely trafficked maritime areas. Data collected from the automatic identification system (AIS) onboard maritime vessels were utilized to analyze dense navigational areas, which were then divided into 1 km grids. Through a spatial-temporal analysis method utilized from The European Marine Observation and Data Network (EMODnet), the occupancy time of the vessels in each grid was calculated to extract dense traffic areas. The dense traffic areas extracted in grid form were processed using the geographical identification system to create polygonal routes by smoothing and simplification. The resulting polygons exhibited different shapes depending on the analysis period. To extract a unique representative route polygon, the CRiteria Importance Through Intercriteria Correlation (CRITIC) method was employed to calculate the shape similarity based on the centroid, shape index, and overlapping area ratio of the polygons. The extracted representative polygon demonstrated the highest shape similarity compared with the other polygons and was utilized by 95.93% of the vessels navigating the analyzed area. The study results can contribute to identifying essential areas for vessels in maritime zones by proposing representative shipping routes.

INDEX TERMS AIS data, CRITIC method, geographical information systems, maritime traffic route, spatial–temporal analysis.

I. INTRODUCTION

The ''Sea Lanes of Communication,'' where maritime transportation occurs, serve as the lifeblood of the logistics industry, transporting essential materials necessary for economic production activities such as oil and various raw materials. With the activation of international trade through maritime routes between nations, maritime navigation and commerce have become essential foundations for national prosperity and the survival of countries with access to the sea [1]. The recent economic development and growth in international trade have led to an increase in the number of maritime vessels, including the vessel traffic volume (VTV), which is associated with ships entering and leaving ports. This indicates the need for improvement, modification, and expansion of shipping routes as well as the optimization of navigation management [2]. Further, the scope for constructing maritime facilities, such as offshore power facilities, aquaculture facilities, submarine cables, and underwater tunnels, is extending globally [3], particularly with the recent construction of large-scale offshore wind power generation sites to secure new energy sources in extensive areas, which

The associate editor coordinating the review of this manuscript and approving it for publication was Yougan Chen.

affects maritime traffic environments [4]. In such an environment, where various political and economic pressures increase in different directions, optimizing shipping routes is essential [5]. Shipping route optimization involves creating a maritime navigation network and establishing fixed routes. Maritime transportation differs significantly from land transportation because ships can navigate freely in all maritime areas in spatial terms. This difference increases the uncertainty of maritime transportation and poses risks to navigational safety [6]. To prevent such risks, international regulations generally stipulate the establishment of navigation plans before a voyage. According to the resolutions put forth by the International Maritime Organization (IMO), voyage planning encompasses the stages of appraisal, planning, execution, and monitoring, all with the approval of the ship's master, covering every phase from berth to berth. Once a voyage plan is permitted, the vessel must navigate in accordance with this plan [7].

The navigation outcomes of vessels can be observed using an automatic identification system (AIS) installed onboard the ships. The results of an analysis of the AIS data can reflect vessel traffic information and can be utilized to establish and manage shipping routes [8]. Numerous studies have analyzed vessel movements using AIS data [9]. AIS data include not only the positional information of ships but also static information related to ship particulars, dynamic information related to navigational status changes, and navigational information related to voyage schedules. AIS data represent a large-scale dataset with millions of data points received daily. As mandated by the IMO, an AIS must be installed in cargo ships engaged in international voyages exceeding 300 gross tons, cargo ships not engaged in international voyages but exceeding 500 gross tons, and passenger ships [10]. Unlike conventional passive methods, such as image-based techniques, which are expensive and time-consuming, an analysis of AIS data received from ships can enable a rapid extraction of their navigation characteristics at a low cost [6]. Recently, there has been an increase in research papers that utilize AIS data to predict future routes [11], [12], [13], [14], additionally, research is being conducted to detect a wide range of ships by complementarily operating Synthetic Aperture Radar (SAR) for ships that are not equipped with AIS, which could be utilized in the future [15], [16]. Thus, shipping routes can be extracted based on AIS data, which sufficiently reflect the trajectories of shipping routes.

Many studies have been conducted on analyzing ship traffic and designing routes based on AIS data. Yu et al. [17] performed optimal route planning at sea to reduce the human errors associated with maritime accidents. They utilized Exploratory Spatial Data Analysis (ESDA) to model ship behavior characteristics (e.g., speed, course), geographical features of ports (e.g., restricted area passages, proper docking), and international regulations (International Regulations for Avoiding Collisions at Sea). Their model presented the most optimal routes with the highest safety and efficiency compared to other studies. Zhang et al. [18] developed an automatic maritime route algorithm by establishing a network with AIS data and IALA-Net. They used the Douglas-Peucker algorithm to form trajectories and extract turning nodes. Subsequently, they derived the optimal route using Ant Colony Optimization (ACO), demonstrating the effectiveness of the algorithm in macro-level traffic flow. Zhang et al. [19] proposed an automatic route design method based on Simple Recurrent Unit (SRU) and AIS data. They analyzed recommended routes, speeds, and paths for different ship types. Notably, they extracted routes using fuzzy adaptive density-based spatial clustering of applications with noise (FA-DBSCAN) by obtaining turning areas of similar routes and linking these areas. Their analysis demonstrated the high accuracy and fast learning speed of the Long Short-Term Memory (LSTM) neural network. Nowy et al. [20] statistically analyzed Świnoujście AIS data to study navigation patterns and model traffic flow. They argued that factors influencing the spatial distribution of ships include ship type, size, and distance to hazards. Their results demonstrated that the standard deviation of traffic flow correlates with the ship size and distance to hazards. Additionally, they analyzed how the location in the waterway varies based on the length of the waterway and the width of navigating ships, indicating its applicability in waterway design and traffic flow modeling.

In existing research, shipping routes are typically extracted in a linear form by connecting berths. However, the actual traffic flow of ships forms a corridor shape with a certain width, rather than a thin line [21]. The World Association for Waterborne Transport Infrastructure (PIANC) has put forth international guidelines on factors constituting shipping routes [22]. For example, PIANC suggests route dimensions as components, including the water depth, route width, and interconnectivity between the vertical and horizontal dimensions. Therefore, shipping routes should be presented in a polygonal shape resembling roads rather than in a linear format connecting points.

A maritime traffic analysis can be conducted using three main methods: grid-based, vector-based, and statistics-based [23]. In vector-based approaches, waypoint extraction is the top priority for analyzing the flow of ship traffic. The waypoints are used to extract traffic patterns, which help perform traffic analysis and prediction [24], [25], [26], [27]. In statistics-based approaches, the ship traffic volume is evaluated quantitatively using statistical methods to derive important traffic parameters or threshold values that can help analyze ship traffic characteristics [28], [29], [30], [31].

To present shipping routes in a polygonal form, the results of shipping activities must be analyzed within specific areas. In this regard, grid-based methods that divide vast marine areas into defined grid cells for analysis can produce favorable results for route presentation. Related studies include those conducted by Yang et al. [32], who utilized nonparametric kernel density estimation methods to calculate the density

of ships in each grid and reflected the impact of the ship size on maritime traffic. Osekowska et al. [33] extracted optimal grid sizes to detect abnormal shipping activities based on potential fields in open seas and near harbors, resulting in grid cells with a size range of 60–200 m near harbors and 300–1000 m in open seas. Kontopoulos et al. [34] detected abnormal ship behaviors by utilizing polynomial interpolation methods to extract normal shipping routes and a modified DB-SCAN algorithm for more consistent route clustering. They subdivided the monitoring area into 0.2° grids for integration with weather services, resulting in the creation of normal route polygons and the detection of abnormal behavior outside these polygons. Kim et al. [35] obtained maritime traffic information for e-navigation purposes by reflecting interpolated AIS data. They calculated the number of ships per grid, generated various traffic data layers, and evaluated the traffic using five gate lines. Lei et al. [36] proposed Maritime Traffic Route Discovery (MTRD) to extract maritime traffic routes that involve AIS pattern mining, pattern summarization, and traffic route generation procedures.

It is essential to present quantitative traffic volume analysis results in the physical space to extract ship traffic concentration areas and conduct quantitative analysis [37]. The quantitative results for each unit area can be obtained by performing calculations using the ship position data, number of ship routes, and ship density in areas divided into grid units. Furthermore, as the size of the AIS data used increases with the duration and scope of the analysis, reducing preprocessing time and enhancing storage capacity become crucial. Wu et al. [38] performed a global density calculation for 33 months (from August 2012 to April 2015) using a grid-based density analysis method in just 56 hours. By selecting an appropriate spatial resolution, it is possible to control the computational load and storage space within reasonable limits [32]. In this regard, grid-based ship traffic analysis can have strengths in the implementation of analysis, results, storage, and result presentation [35].

Shipping routes can be utilized in various ways by stakeholders. As a type of spatial data, shipping routes can be managed using Geographic Information Systems (GIS). For SOLAS-regulated vessels, the use of an Electronic Chart Display and Information System (ECDIS) is mandatory. On the other hand, marine developers and users of maritime areas can employ GIS software like ArcGIS, developed by Esri, or QGIS, an open-source GIS software. To transform grid-based ship activity area analysis results into route shapes for use in GIS, vector-based algorithms are necessary. These algorithms facilitate the conversion of spatial data formats, enabling accurate and efficient representation of shipping routes in GIS platforms [39], [40]. To smooth shipping routes, Yun et al. [41] utilized smoothing algorithms, whereas Li and Zhang [42] optimized nearby ship tracks using the Bézier curve. Lee and Cho [43] extracted simple routes without intersections by enhancing the Douglas–Peucker algorithm to simplify shipping routes. Wei et al. [44] combined the Douglas–Peucker algorithm with the sliding window algorithm to simplify routes that reflect ship behavior. Consequently, dense ship traffic areas in grids can be smoothed and simplified into route shapes using vector-based algorithms.

However, the duration and scope of the data for extracting existing maritime routes vary among existing studies, and shipping activities can differ depending on various factors over time. Therefore, a procedure is required to select representative routes among the extracted ones.

Representativeness fundamentally relies on similarity, which is a topic that has received attention not only from psychologists but also from computer scientists and related researchers [45]. In this paper, we propose a solution to this problem. Methods for measuring the similarity in spatial data include geometric, topological, and semantic methods [46]. Geometric methods, which utilize the distances, bearings, positions, and shapes between spatial data, are most commonly used [47], [48], [49], [50].

When utilizing geometric methods, the final similarity is determined based on various criteria, requiring the definition of relationships among these criteria and the calculation of weights using multi-criteria decision-making (MCDM) methods. An objective MCDM method, which excludes the decision-maker's judgment, is needed [51]. Examples include entropy-based methods [52], [53], CRiteria Importance Through Inter-criteria Correlation (CRITIC) [54], FANMA methods [55], and Data Envelopment Analysis (DEA) [56]. The entropy method determines objective criterion weights based on the concept of entropic grading of data in the decision matrix. The FANMA method calculates criterion weights using principles of distance from an ideal point and early-time weight normalization. The DEA method calculates weights by solving a linear optimization model for each alternative and measuring their efficiency against defined criteria. The CRITIC method uses standard deviation to calculate criterion values per column option and determines criterion contrasts using the correlation coefficients of all column pairs.

Previous studies argue that among various MCDM methods, the CRITIC method is the most widely applied and objective [57], as it considers both the intensity of contrasts and trade-off relationships among decision criteria, providing additional advantages. For instance, Kim et al. [58] and Kim et al. [59] extracted geometric similarity of area objects and calculated the final shape similarity using CRITIC. Therefore, this study will refer to previous research and employ the CRITIC method to calculate the weights final shape similarity.

Kim et al. [58] assessed the similarity by calculating the position criterion, shape criterion with a shape index, and area criterion to determine the duplication area ratios between digital topographic map and street-name address base map. The CRiteria Importance Through the Intercriteria Correlation (CRITIC) method was employed by considering the standard deviation and correlation between criteria to

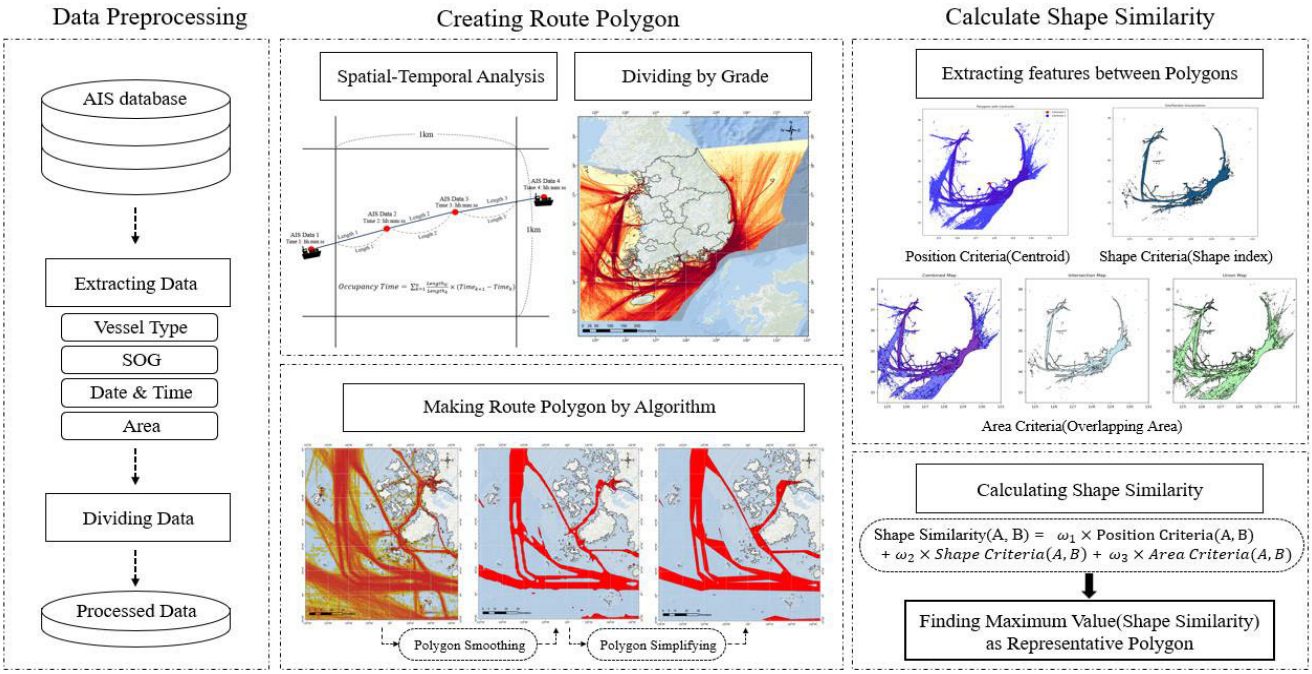

FIGURE 1. Overview of the methodology used in this study to find representative maritime routes.

detect the similarity between the polygons. Ultimately, the shape similarity between each pair of polygon objects can be extracted, enabling various applications.

In this study, we aimed to extract representative shipping routes in South Korea. Through a grid-based spatial-temporal density analysis within the Korean Exclusive Economic Zone (EEZ), we calculated the vessel occupancy time in each grid and extracted areas where ships conventionally navigate. Based on the calculated occupancy time, we classified dense navigational areas into grades. Next, we utilized vector-based algorithms to extract these grid-based dense navigational areas into polygonal shapes resembling routes. The extracted polygons were evaluated for the shape similarity between each pair, and the polygon with the highest shape similarity within each grade was taken as the representative shipping route for South Korea. By presenting major shipping routes, we aim to prevent indiscriminate marine development by maritime users who encroach upon critical navigation areas. Additionally, we seek to designate essential areas for ship navigation, thereby ensuring safe shipping lanes.

The rest of this paper is organized as follows: Section II provides a general overview of this study, including data collection, analysis area, spatial-temporal density analysis, vector-based algorithms, and a methodology for the shape similarity analysis. Section III presents the detailed analysis results. Section IV explains the significance of the research. Finally, Section V presents the conclusions.

II. MATERIALS AND METHODS

A. OVERVIEW OF STUDY

Fig. 1 presents the main flowchart of this study. To present dense ship traffic areas as routes, the initial step involved preprocessing the AIS data using Python. The analysis area was divided into grids, and the vessel occupancy time within each grid was calculated using Structured Query Language (SQL). Next, using ArcGIS Pro version 3.2.1, a proprietary GIS software developed by Esri, the occupancy time was categorized into grades. Grid-based dense areas were then transformed into polygons using specific algorithms within the software. These polygons were then compared based on their characteristics to calculate the shape similarity. The polygon with the highest shape similarity was selected as the representative route.

B. DATA PREPROCESSING

The AIS data were collected from the General Information Center on Maritime Safety and Security (GICOMS) operated by the Ministry of Oceans and Fisheries of the Republic of Korea. The AIS data contain dynamic information such as the location, time, speed, and course, as well as static information, including the Maritime Mobile Service Identity (MMSI) number, International Maritime Organization (IMO) number, ship type, ship length, and ship width. This information can be categorized based on the area, period, ship type, size, speed, and status through preprocessing.

Because the GICOMS data encompassed all the surrounding waters of Korea, no additional designation was necessary for the analysis area. The analysis period was from January to December 2020 and was categorized on a monthly basis. Ships are typically classified based on their cargo type. In South Korea, the most commonly operated ships are cargo ships transporting heavy goods (by weight), such as general cargo ships and tankers, and cargo ships transporting bulk goods (by volume), such as container ships, roll-on/roll-off

(RoRo) ships, car carriers, liquefied petroleum gas (LPG) ships, and liquefied natural gas (LNG) ships. Accordingly, the selected ship categories were general cargo and tanker ships. For vessel size, no specific size limitations were set in order to utilize data from all cargo ships and tanker vessels. To extract dense ship traffic areas, it is necessary to remove the data when the ships are stationary, mooring, or anchored. According to the International Telecommunications Union (ITU) technical standard [60], for Class-A ships, the transmission rate of AIS data is determined based on the dynamic information status and speed, as listed in Table 1. In this study, data from ships with speeds below 3 knots were removed to include data only when the ships were in operation. Table 2 presents an overview of the AIS data used in this study.

TABLE 1. Reporting intervals of class-A shipborne mobile equipment.

Ship's Dynamic Conditions	Reporting Interval
Ships anchored or moored and not moving faster than 3 knots	3 min
Ships anchored or moored and moving faster than 3 knots	10 s
Ships with speeds ranging from 0 to 14 knots	10 s
Ships with speeds ranging from 0 to 14 knots and changing course	3 1/3 s
Ships with speeds ranging from 14 to 23 knots	6 s
Ships with speeds ranging from 14 to 23 knots and changing course	2 s
Ship speed > 23 knots	2 s
Ships with speeds > 23 knots and changing course	2 s

TABLE 2. Overview of the AIS data used in this study.

Category	Area	Periods	Type	Length	Speed
Range	All coastal areas	1st. Jan. 2020. to 31st. Dec. 2020.	Cargo and tanker	All length of vessels	Above 3 knots

C. CREATING ROUTE POLYGON

To extract shipping routes, it is necessary to identify areas in which ships conventionally navigate. Grid-based methods can also be used for spatial extraction. The grid-based method involves dividing an analysis area into polygons of a specific size and inputting the characteristic values into each grid. In this study, we applied a method for calculating the time ships spent in specific grids, referred to as the grid occupancy time calculation. This method, which is adopted by The European Marine Observation and Data Network to create ship density maps for EU waters, offers advantages such as accurate density analysis and visualization without requiring data interpolation or parameter settings [37].

Since the AIS data comprises continuous time-series with temporal attributes that connect the data points of a single ship to reveal its trajectory, overlaying this trajectory onto a grid allowed us to determine whether each data point fell within or outside the grid. For points that fell within the grid, the occupancy time between the points could be calculated by determining the time difference. For points falling outside the grid, we could determine the distance ratio between the point, intersection of the trajectory with the grid, and another point. This distance ratio provides the time ratio between the point, intersection of the trajectory with the grid, and other points, enabling the calculation of the occupancy time within the grid. Fig. 2 shows this process. The grid size selected in this study was 1 km × 1 km, based on previous research and regulations in Korea and the EU [61], [62].

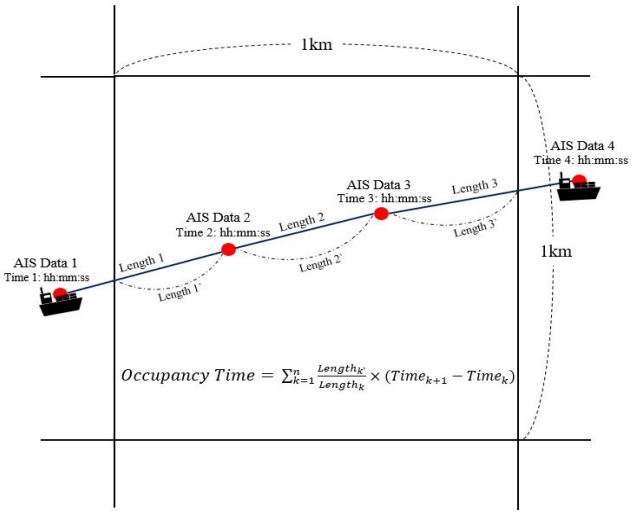

FIGURE 2. Spatial-temporal analysis method.

To extract shipping routes, it is essential to identify grids with high occupancy times. For this extraction, percentiles representing the characteristics of the positions of data values can be utilized [63]. Among percentiles, quartiles are the most common; there are also quantiles and deciles for finer granularity. In this study, the ship occupancy times were classified based on percentiles.

The occupancy times for each grid were extracted based on percentiles ranging from the top 10% to 50%. As a result, five datasets were constructed for each month, yielding 60 spatial-temporal density analysis datasets over the course of one year. The occupancy time data, divided into quantile units, remained in a grid-based format. This format forms a

checkerboard-shaped polygon, which is difficult to define as a shipping route. The routes should be continuous polygons; therefore, nearby polygons must be merged first. This was done using the aggregate polygon algorithm in the ArcGIS. The algorithm combines polygons within a specified distance into a new polygon. Hence, it can easily create a polygon from orthogonal or nonorthogonal polygons. The specified distance was set to 1 km, which was the same as the grid size.

The initial number of grid cells was 408,566, and the average number of polygons reduced for each percentile after applying the algorithm, as shown in Table 3. The reduction percentage increases from the Upper 10% to 40% and then slightly decreases. This is because more grids are selected and combined into polygons in the higher percentiles, resulting in a decrease in the total number of polygons.

TABLE 3. Reduction percentage after aggregate polygon.

Percentile	Upper 10%	Upper 20%	Upper 30%	Upper 40%	Upper 50%
Average counts	402	691	774	868	732
Reduction Percentage(%)	0.098	0.169	0.190	0.212	0.179

The aggregate polygon algorithm results in polygons with empty spaces inside, because it merges only the grids within a specified distance (1 km). Polygons with numerous empty spaces bring difficulties in creating linear and continuous polygons. Therefore, the polygon elimination algorithm was employed to delete small empty spaces inside the polygons (see Fig. 3). The resulting polygons showed an improvement in the shape without any difference in the number of polygons.

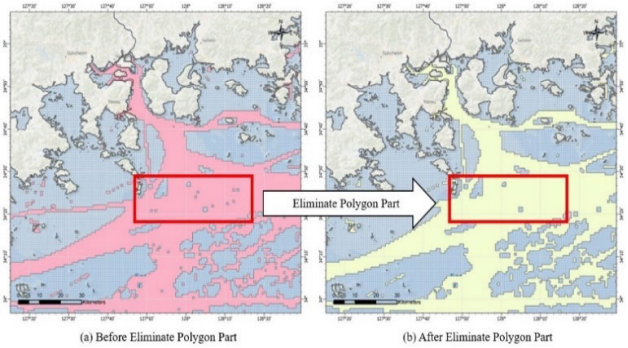

FIGURE 3. Result of polygon elimination algorithm.

The edges of the polygons resulting from the polygon elimination algorithm maintained a grid-based polygonal shape, requiring further smoothing for refinement. Two commonly used algorithms for smoothing polygons are polynomial approximation using an exponential kernel (PAEK) and Bézier interpolation [64], [65]. The PAEK method utilizes parametric continuous averaging to compute smoothed lines, in which coordinates at a given distance along the parameter are weighted-averaged to form new coordinates.

Conversely, the Bézier method fits the Bézier curves through all the segments of the input line, resulting in a smooth curve at each vertex. However, the Bézier algorithm tends to generate excessive polygons by crossing the existing grid boundary areas and may not work effectively in the case of narrow coastal or strait areas, as shown in Fig. 4a. By contrast, the PAEK algorithm allows users to specify parameters for appropriate smoothing as shown in Fig. 4b. Larger parameters result in smoother lines; however, excessively large settings may not adequately reflect the original polygons and may lead to coastal encroachment. Therefore, the PAEK algorithm was selected to smooth each polygon using a parameter value of 5 km as the optimal value for smoothing, in which case there is no land encroachment.

After applying the PAEK algorithm, the polygons still exhibit irregular edges. Internationally designated maritime zones such as Traffic Separation Schemes and harbor approach channels are uniformly delineated with flat edges. In the context of maritime routes, which serve as pathways for vessel navigation, it is imperative to consider straightening rather than maintaining irregular boundaries lsuch as those observed in the Traffic Separation Schemes and channels. Therefore, to form routes that lead to straight sections, the polygons need to be simplified. To achieve this, a simplification algorithm was utilized to derive the straight sections of the polygons from their original form as shown in Fig. 5. Simplification algorithms primarily use four methods. Each algorithm operates by removing unnecessary vertices while maintaining the essential shape of the polygons. The Douglas and Peucker algorithm identifies and removes redundant vertices to simplify the data [66]. The Wang and Muller algorithm identifies and eliminates insignificant bends to simplify the data for display at smaller scales [67].

The Zhou–Zones algorithm identifies valid triangular areas for each vertex, assigns weights to each triangle, and then removes vertices to simplify the data while preserving as many characteristics as possible [68]. The Visvalingam–Whyatt algorithm identifies triangles for each vertex and removes vertices to maintain as many features as possible while simplifying the data. After algorithm application, it was observed that the Visvalingam and Whyatt and Zhou–Zones algorithms still produced rounded polygon edges, which were deemed unsuitable for the final polygon shape [69]. Conversely, the Douglas–Peucker and Visvalingam–Whyatt algorithms generated straighter lines, making them suitable for the final polygonal shape. To determine the more appropriate algorithm, the results were quantitatively compared.

The quantitative comparison involved comparing the overlapping areas between the resulting polygons and the South Korean territory. The algorithm that resulted in fewer overlapping areas was selected. The average values of the overlapping areas for each month were categorized into grades. The results indicated that the Visvalingam–Whyatt algorithm was the most suitable, as shown in Table 4.

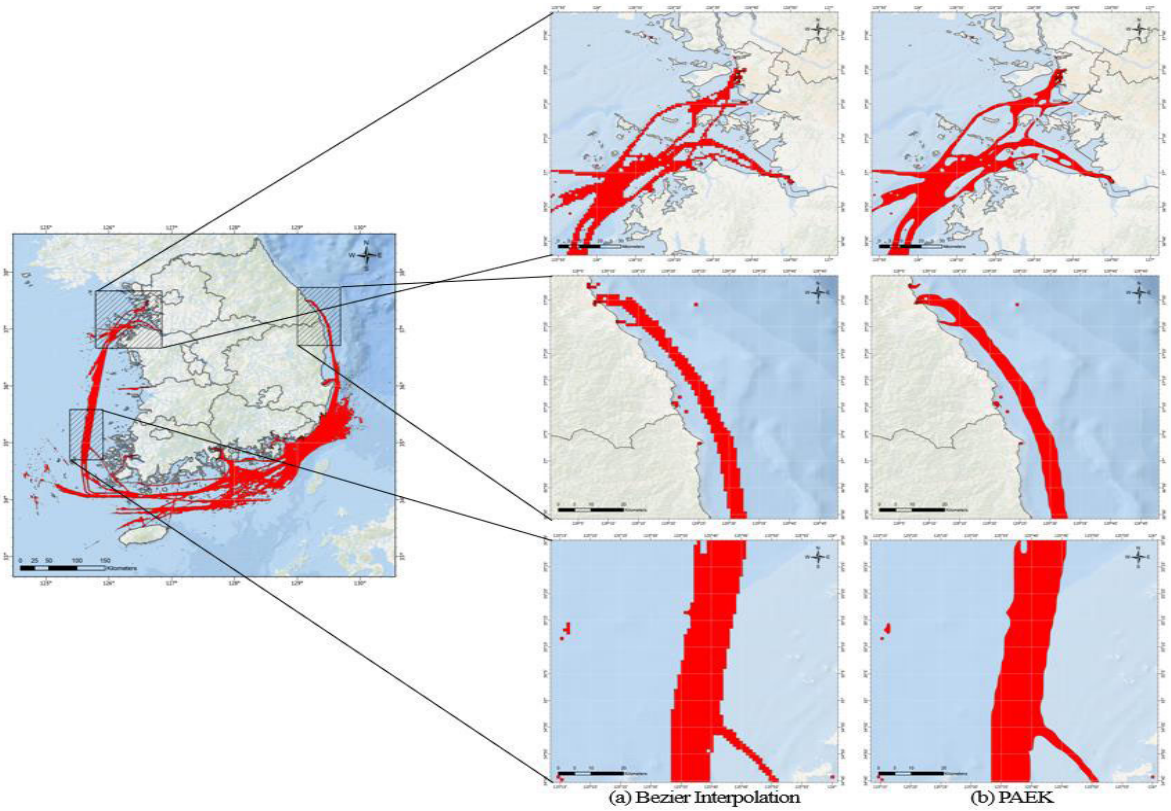

FIGURE 4. Results of smoothing polygon algorithms.

D. CALCULATION OF SHAPE SIMILARITY

Using the aforementioned algorithms, we conducted a monthly vessel occupancy time analysis and extracted route polygons for dense traffic areas based on percentiles. The vessel traffic volume exhibited a complex nonlinear pattern influenced by port service indices, incidents, and weather conditions, making prediction challenging [2]. Consequently, route polygons for each month and percentile may display varying density shapes depending on the circumstances at the time. Therefore, it is necessary to extract representative polygons that can be used as routes.

To achieve this, the similarity between polygons must be determined to designate the polygon with the highest similarity as the representative one. Because polygons extracted through the algorithm do not contain specific attribute information, geometric methods, such as the distance, shape, and area of the polygons, are the most useful for similarity measurements. In this study, geometric information was extracted from the polygons to measure their similarity.

The first extracted information was based on the position criterion, where the centroids of the polygons were identified, and the distances between the centroids were compared. To compare Polygons A and B, the coordinates of their centroids (x, y) were identified, and the distance was calculated using the Euclidean distance formula. Subsequently, normalization was performed using the maximum value of the distance between the centroids, as shown in Equation (1). A higher normalized value (closer to 1) indicates a greater similarity between the corresponding objects.

$$Position\ Criterion = 1 - \frac{P_A, P_B}{\max\left(P_{Aall}, P_{Ball}\right)} \tag{1}$$

Here, (P_a, P_b) represents the Euclidean norm to calculate the distance between the centroid of Polygons A and B.

The second piece of information is extracted based on the shape criterion. According to Burghardt and Steiniger, a positive correlation exists between the area and perimeter of polygonal objects [70]. They further suggested a positive correlation between the size (area and perimeter) and shape index. When the area and perimeter are large, the shape index increases. Hence, the shape criterion is calculated by obtaining the shape indices of target Polygons A and B and normalizing the difference value. Similar to the position criterion, a higher result indicates a greater similarity in the shape between the two objects.

$$SI_{dif}\ (A, B) = \left| \frac{P_A}{2\sqrt{\pi A_A}} - \frac{P_B}{2\sqrt{\pi A_B}} \right| \tag{2}$$

$$Shape\ Criterion = 1 - \frac{SI_{dif}\ (A, B)}{\max\left(SI_{dif}\ (A_{all}, B_{all})\right)} \tag{3}$$

Here, SI_{dif} represents the difference in the shape index between the two objects, where P denotes the perimeter of each object, and A represents the area of each polygon object.

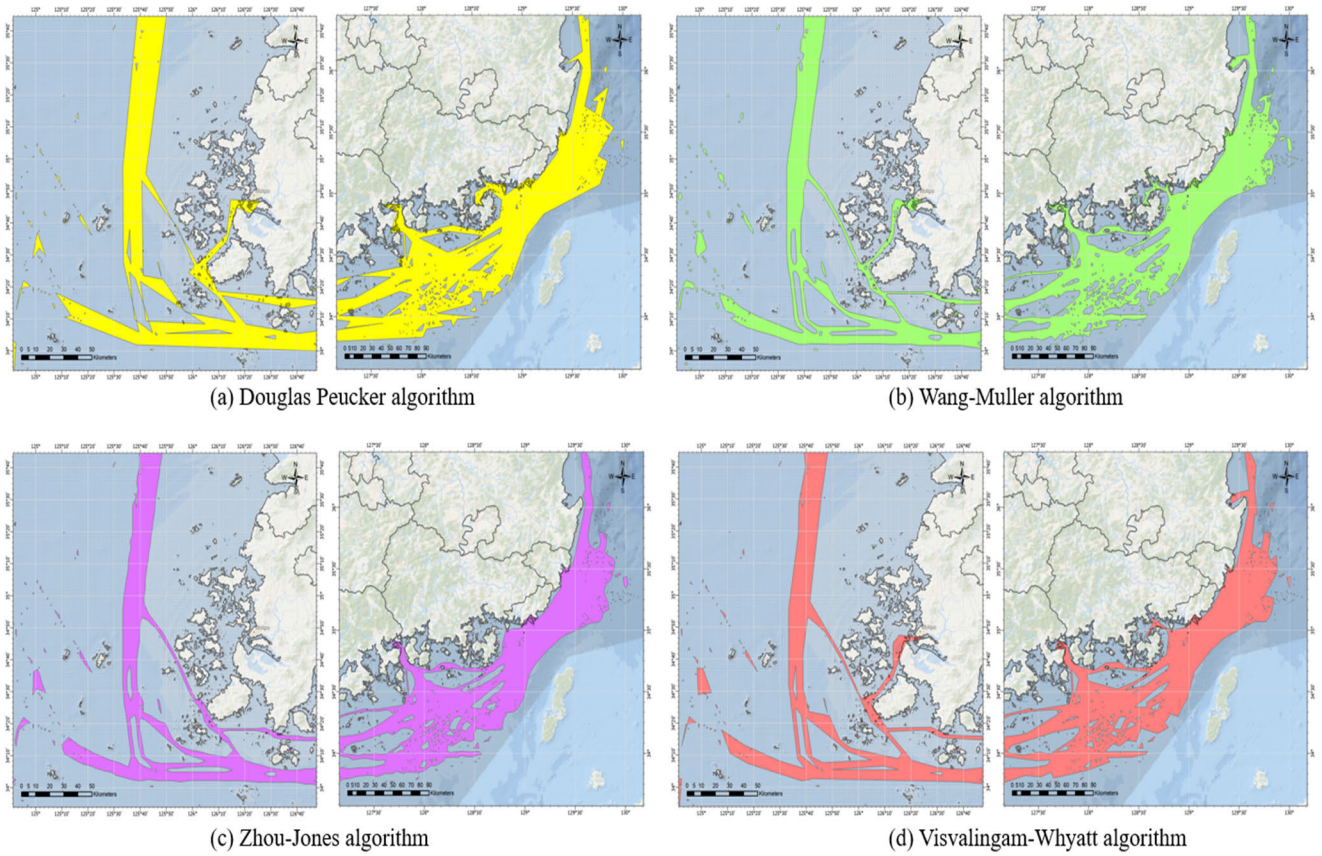

FIGURE 5. Results of polygonal simplification algorithms.

The third piece of information is extracted based on the area criterion. The area criterion utilizes the symmetric difference between two polygons and is calculated by subtracting the overlapping values from the areas of the two polygons. As the overlapping area between the polygons increases, the symmetric difference decreases. The overlapping area ratio is defined as the symmetric difference subtracted from the sum of the areas of the polygon object pair divided by the total area of the two polygons. Normalization is achieved using the maximum value of the overlapping area ratio. Similar to the other criteria, a higher value of the area criterion indicates a greater similarity in the area ratio between the polygons.

$$OA\,(A_A, A_B) = \left| \left(A_{(A \cup B)} - \frac{A_{(A \cap B)}}{A_A + A_B} \right) \right| \tag{4}$$

$$\text{Area } Criterion = 1 - \frac{OA\,(A_A, A_B)}{\max\,(OA\,(A_{Aall}, B_{Aall}))} \tag{5}$$

where $OA\,(A, B)$represents the overlapping area ratio, which is calculated as the symmetric difference between the areas of Polygons A and B. The variable A represents the area of each matching polygon.

In multicriteria decision making, where various criteria are used to select the optimal alternative, the method of simply averaging or using the standard deviation has limitations, as it assigns equal weights to all criteria and does not consider the interrelationships between them [71]. Therefore, in this study, we intended to use the CRITIC method proposed by Diakolulaki et al. to determine the weights by considering the standard deviation and correlations of each criterion and to derive combinations of criteria [54].

TABLE 4. Overlapped areas(km2) with territory.

Percentile	Upper 10%	Upper 20%	Upper 30%	Upper 40%	Upper 50%	Selected Algorithm
Douglas–Peucker	133.4	186.9	249.8	330.6	481.6	
Visvalingam–Whyatt	**127.8 (Lower)**	**178.0 (Lower)**	**223.5 (Lower)**	**310.4 (Lower)**	**452.8 (Lower)**	**Selected**

In the CRITIC method, the weights of each criterion are calculated based on the information content, standard deviation, and correlation between matching criteria rather than relying on subjective judgments. The computed weights are then applied to each criterion to calculate the final shape similarity value. A value closer to 1 indicates a higher degree of similarity between two objects. To compute the CRITIC, standardization is performed for each interacting criterion,

and correlation coefficients are calculated between the interacting criteria. The amount of information is determined using the correlation coefficients and standard deviations of each criterion, leading to the computation of the final weights for each criterion.

Ultimately, when measuring the shape similarity between different polygons for each route grade, the polygons with the highest average shape similarity are selected as representative route polygons.

$$W_j = \frac{C_j}{\sum_{k=1}^{m} C_k}, \quad C_j = \sigma_j \times \sum_{k=1}^{m} \left(1 - r_{jk}\right) \tag{6}$$

$$\begin{aligned} &\textit{Shape Similarity}\,(A, B) \\ &= w_1 \times \textit{Position Criterion}\,(A, B) \\ &\quad + w_2 \times \textit{Shape Criterion}\,(A, B) \\ &\quad + w_3 \times \textit{Area Criterion}\,(A, B) \end{aligned} \tag{7}$$

Here, C_j represents the amount of information for each matching criterion, σ_j is the standard deviation of each matching criterion, and r_{jk} denotes the correlation coefficient between matching criteria.

III. RESULTS

A. EXTRACTION OF POLYGON ROUTE

Fig. 6 presents the calculated occupancy times for each percentile resulting from the spatial-temporal density analysis. The occupancy time was computed by summing the attribute values of the occupancy times within the selected grids, dividing by percentiles, and measuring in hours. The total occupancy time analysis revealed that March had the highest occupancy time, whereas November had the lowest. The occupancy time of ships per grid was divided into 10 grades, and Fig. 7 depicts the results with a gradual color scale applied. It can be observed that the vessels navigate through almost all the maritime areas of South Korea, and that the dense traffic areas are not limited to specific regions but are connected in the form of lines.

After the application of the polygonization algorithm to the results of the spatial-temporal density analysis, the calculated occupancy time grids could be extracted in a linear polygonal form (see Fig. 8). The upper 10% percentile route polygons clearly demonstrate a dense flow of domestic vessel traffic. In particular, routes entering and exiting major ports in Korea, such as Incheon, Busan, Yeosu, Gwangyang, Ulsan, and Mokpo, could be clearly identified. In addition, traffic separation scheme (TSS) and other legally designated routes accurately reflected traffic flows, enabling route construction. The upper 20% and 30% percentile polygons better represent international routes than the upper 10% percentile polygons. The routes between Korea and China, Singapore, and the trans-Pacific routes to the United States are clearly visible. However, polygons with percentiles higher than 40% cover excessively wide areas, which may pose challenges for their utilization as routes.

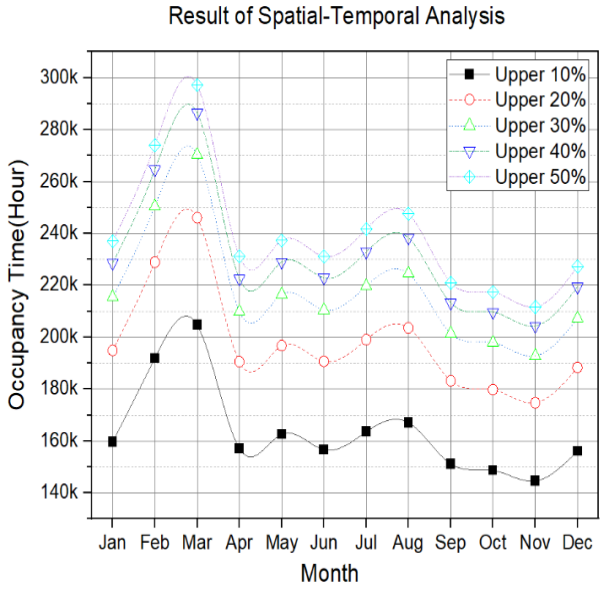

FIGURE 6. Result of spatial-temporal analysis.

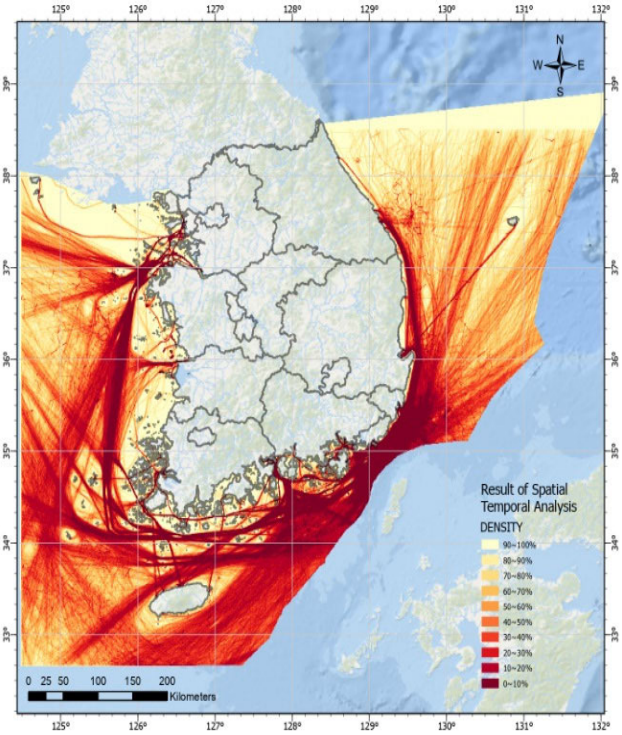

FIGURE 7. Spatial-temporal analysis result.

B. ROUTE ESTIMATION

The results of the spatial-temporal density analysis, extracted into polygons through algorithms, allowed for the representation of vessel routes closer to straight lines and facilitated visualization. It is essential to verify whether the analysis results extracted for the density adequately reflect the VTV. To assess the extent to which the density analysis results, represented by both the grid-based polygons and the polygons

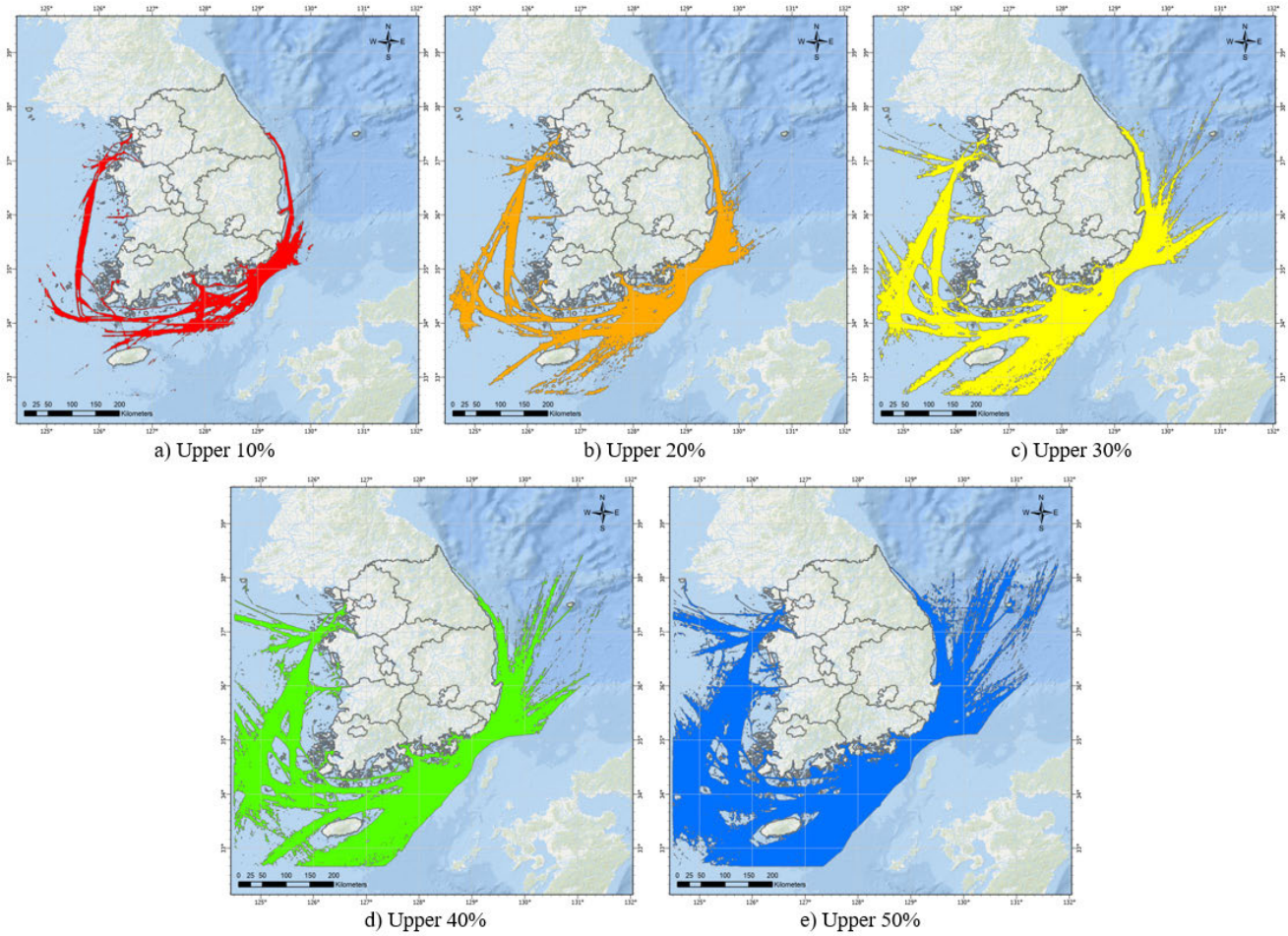

FIGURE 8. Route polygon maps after the application of algorithm.

after applying the algorithm, reflect the VTV, a data rate analysis was conducted based on the number of AIS data points (see Table 5). The results indicated that after applying the algorithm, the polygons reflected, on an average, 1.1% more vessel data than grid-based polygons, demonstrating that polygon-based routes capture more traffic.

$$Data\ Rate = \frac{AIS\ Data\ Counts\ in\ \ Polygon}{Total\ AIS\ Data\ Counts\ for\ each\ Month} \times 100\,(\%) \quad (8)$$

According to the criteria outlined in a report jointly published by the UK Department of Trade and Industry, Department for Transport, and Maritime and Coastguard Agency each route should accommodate 95% of vessel traffic [72].

Moreover, it is recommended to consider any variation in the traffic by incorporating a standard deviation of ±2. Therefore, routes reflecting approximately 93%–97% of the traffic would be considered appropriate. To verify whether the routes extracted after applying the algorithm adequately reflected vessel traffic, the following formula was used:

$$Coverage\ Rate = \sum_{k=1}^{n} \frac{P_c\,(r_k)}{P\,(r_k)} \times 100\,(\%) \quad (9)$$

Here, $P_c\,(r_k)$ represents the percentage of vessels contained within route r_k, and $\mathrm{P}\,(r_k)$ represents the number of vessels

TABLE 5. Data rate differences between polygon and grid based methods.

Percentile	Polygon-Based (a)	Grid-Based (b)	Difference (a)-(b)
Upper 10%	61.63	60.68	0.95
Upper 20%	76.60	75.25	1.35
Upper 30%	85.05	83.72	1.33
Upper 40%	90.01	89.11	0.90
Upper 50%	93.24	92.22	1.02
Average	81.31	80.20	1.11

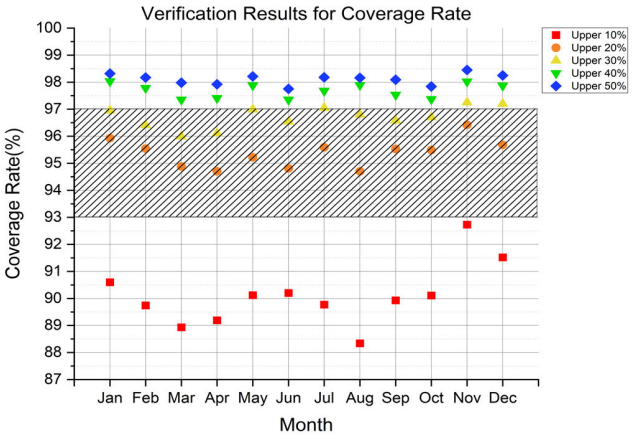

FIGURE 9. Verification results for coverage rate.

TABLE 6. Coverage rate analysis.

Percentile	Upper 10%	Upper 20%	Upper 30%	Upper 40%	Upper 50%
Coverage Rate Average (%)	90.10	95.37	96.71	97.68	98.11
Counts within Coverage Rate	0	12	9	0	0

TABLE 7. Criterion standard deviation.

Category	Position Criterion	Shape Criterion	Area Criterion
Standard Deviation	0.207	0.211	0.257

TABLE 8. Correlation for each criterion.

Category	Position Criterion	Shape Criterion	Area Criterion
Position Criterion	1	0.046	0.030
Shape Criterion	0.046	1	0.648
Area Criterion	0.030	0.648	1

passing through each route in the Korean area on a monthly basis. Fig. 9. presents the verification results, indicating that the upper 20% percentile route appropriately reflects the traffic volume and Table 6 presents the number of polygons whose coverage rate is within the range at each percentile.

C. RESULT OF SHAPE SIMILARITY

After applying the algorithm and extracting the route polygons, the shape similarity was calculated based on these polygons. The position, shape, and area criteria were computed for all the route polygons using Equations 1, 2, and 3, respectively. Table 7 and Table 8 present the standard deviations and correlation coefficients for each criterion. The final weights W_j were calculated using Equation (4). Table 9 presents the results.

TABLE 9. Weights for each criterion.

Category	$\sum_{k=1}^{m}(1-r_{jk})$	σ_j	C_j	W_j
Position Criterion	1.923	0.207	0.397	0.393
Shape Criterion	1.305	0.211	0.276	0.272
Area Criterion	1.321	0.257	0.339	0.335

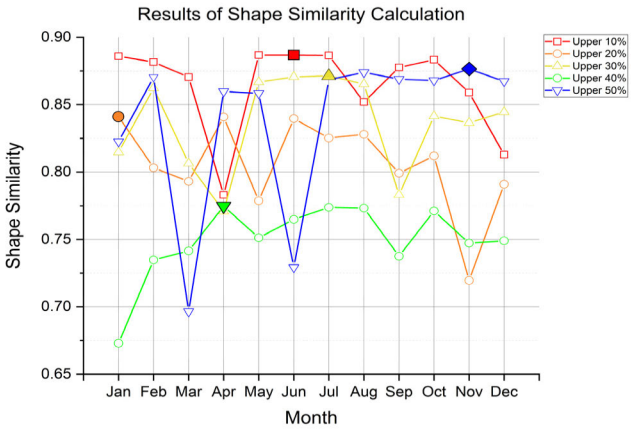

FIGURE 10. Results of shape similarity calculation.

TABLE 10. Shape similarity result analysis.

Percentile	Upper 10%	Upper 20%	Upper 30%	Upper 40%	Upper 50%
Shape Similarity Avgerage	0.864	0.806	0.836	0.749	0.838
Maximum Shape Similarity	0.887	0.841	0.871	0.775	0.876
Month	Jun	Jan	Jul	Apr	Nov

The shape similarity between the route polygons was computed based on the calculated weights for each matching criterion. The average shape similarity between route polygons was calculated for each month and percentile. An average shape similarity value closer to 1 indicates a greater similarity with the other polygons, suggesting its suitability as a representative polygon. Fig. 10 illustrates the shape similarity of various polygons, with the highest value indicated by a filled marker on the graph. The shape similarity was the highest in the upper 10%, with an average of 0.864, and was the lowest in the upper 40%, with an average of 0.749. Among all the polygons, the one with the highest shape similarity was the January polygon in the upper 10%, showing a shape similarity of 0.887, as shown in Table 10.

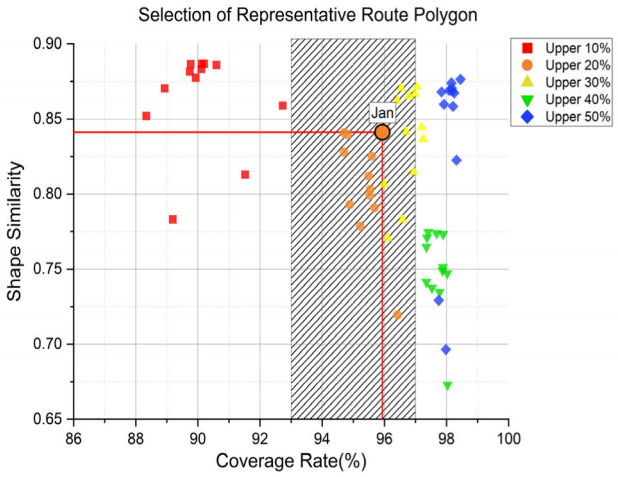

FIGURE 11. Selection of representative route polygon.

D. FINAL REPRESENTATIVE ROUTE POLYGON SELECTION

Ultimately, considering both Coverage Rate and Shape Similarity, the representative polygon was selected as the January polygon of the upper 20% (see Fig. 11). All the polygons in the upper 20% range are suitable for presenting as corridors with a VTV accommodation of 93%–97%. Among these, the January polygon, which presents a Shape Similarity of 0.841, is selected as the most appropriate representative polygon. Conversely, the polygons in the upper 10% do not satisfy the VTV standards required for corridor suitability. The upper 40% and upper 50% polygons accommodate nearly all the VTVs, indicating that they encompass excessively broad areas as corridors. Although 75% of the traffic routes in the polygons upper 30% adequately reflect the appropriate VTV, the July polygon, which presents the highest Shape Similarity, exceeds 97% VTV, rendering it unsuitable. Therefore, the January polygon of the upper 20% is proposed as the final representative polygon, as illustrated in Fig. 12.

IV. DISCUSSION

The changing maritime traffic environment, coupled with the increase in international trade volume, emergence of new vessel types, and the establishment of maritime power facilities, necessitates the continuous evolution of maritime traffic management to ensure the safe navigation of vessels. The construction of navigational routes in the form of maritime traffic routes based on precise polygon shapes is essential for the effective management of maritime traffic. However, in Korea, safe and economically viable routes for cargo ships are yet to be established.

Previous studies have analyzed maritime traffic based on large-scale AIS data, employing grid-, vector-, and statistics-based approaches to extract dense shipping activity areas or major waypoints for network construction. However, the results of these analyses do not consistently yield accurate polygonal routes, and the variability in the data used for the analysis can lead to inconsistent findings over time.

In this study, we selected route polygons that sufficiently reflected the vessel traffic volume and represented

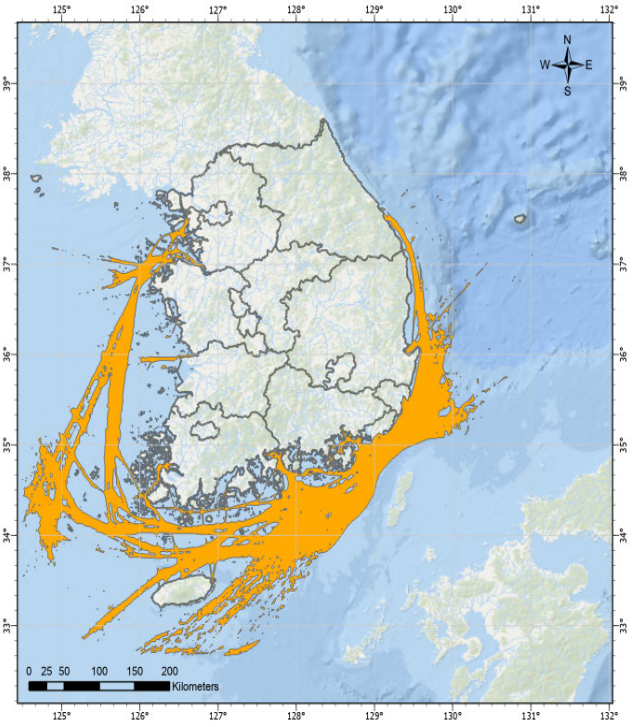

FIGURE 12. Final representative polygon route in south korea.

all the periods used in the analysis. Using the EMODnet method, we calculated the vessel occupancy time through a grid-based approach. Subsequently, we classified the grid-shaped vessel occupancy times into percentile categories and extracted the straight-line routes by smoothing and simplifying the grid-based analysis results using a vector-based algorithm, in ArcGIS. To select a representative polygon, we calculated the shape similarity between all the route polygons based on their shapes. The polygon with the highest similarity was selected as the representative polygon in each percentile. To calculate the shape similarity, we analyzed the shape similarity using the CRITIC method based on the location criterion with centroid, shape criterion with the shape index, and overlapping area ratio criterion.

The results indicated that the upper 20% and upper 30% routes could accommodate 93%–97% of the vessel traffic. Among these, the upper 20% route in January demonstrated the highest shape similarity of 0.841, making it the most suitable route. Through this study, we proposed routes for cargo ships in Korean waters that can be used for safe and economical voyage planning while entering or navigating Korea. Moreover, the standardized extraction criteria and methods used in the route selection and planning for Korea can be utilized for other regions of the world, and the clear delineation of areas into polygons makes it easier to reflect the changes in maritime traffic.

V. CONCLUSION

This study aimed to extract representative routes that sufficiently reflected maritime traffic in Korean waters. Through

a spatial-temporal density analysis, the vessel occupancy time was calculated for each grid. Using the ArcGIS, we applied an algorithm to convert the calculated occupancy time into route polygons, and demonstrated that the extracted routes could accommodate 95% of the vessel traffic in the area. Further, by comparing route polygons based on the location, shape, and overlapping area ratio criterion, we identified the most similar route polygon as the representative route.

This study has a few limitations. First, we focused on cargo and tanker ships; the activities of other types of vessels were neglected. The traffic routes of passenger ships and fishing vessels differ in purpose from those of cargo ships. In the case of fishing vessels, it is necessary to use V-PASS data instead of AIS data, which implies that a different analytical approach is required. Second, the uniformity of the proposed route widths may require further improvement through additional studies. Future research should extend the scope to include more types of vessels and conduct studies to enhance the route width and shape and improve the effectiveness of the research findings.

REFERENCES

[1] S.-H. Jang, "Intimidation over SLOC and the method to ensure safety," *Korean J. Political Sci.*, vol. 23, no. 3, pp. 239–257, 2015.

[2] G. Su, T. Liang, and M. Wang, "Prediction of vessel traffic volume in ports based on improved fuzzy neural network," *IEEE Access*, vol. 8, pp. 71199–71205, 2020.

[3] A. B. Bugnot, M. Mayer-Pinto, L. Airoldi, E. C. Heery, E. L. Johnston, L. P. Critchley, E. M. A. Strain, R. L. Morris, L. H. L. Loke, M. J. Bishop, E. V. Sheehan, R. A. Coleman, and K. A. Dafforn, "Current and projected global extent of marine built structures," *Nature Sustainability*, vol. 4, no. 1, pp. 33–41, Aug. 2020.

[4] Q. Yu, K. Liu, A. P. Teixeira, and C. G. Soares, "Assessment of the influence of offshore wind farms on ship traffic flow based on AIS data," *J. Navigat.*, vol. 73, no. 1, pp. 131–148, Jan. 2020.

[5] M. H. Moradi, M. Brutsche, M. Wenig, U. Wagner, and T. Koch, "Marine route optimization using reinforcement learning approach to reduce fuel consumption and consequently minimize CO_2 emissions," *Ocean Eng.*, vol. 259, Sep. 2022, Art. no. 111882.

[6] Z. Liu, H. Gao, M. Zhang, R. Yan, and J. Liu, "A data mining method to extract traffic network for maritime transport management," *Ocean Coastal Manage.*, vol. 239, May 2023, Art. no. 106622.

[7] *Guideline for Voyage Planning*, IMO, London, U.K., Nov. 1999, vol. 893, no. 21.

[8] L. Fan, W. W. Wilson, and D. Tolliver, "Optimal network flows for containerized imports to the united states," *Transp. Res. E, Logistics Transp. Rev.*, vol. 46, no. 5, pp. 735–749, Sep. 2010.

[9] M. Christiansen, E. Hellsten, D. Pisinger, D. Sacramento, and C. Vilhelmsen, "Liner shipping network design," *Eur. J. Oper. Res.*, vol. 286, no. 1, pp. 1–20, 2020.

[10] International Maritime Organization. (Nov. 1974). *International Convention for the Safety of Life at Sea (SOLAS)*. [Online]. Available: http://www.imo.org/About/Conventions/ListOfConventions/Pages/International-Convention-for-the-Safety-of-Life-at-Sea-%28SOLAS%29,-1974.aspx

[11] X. Zhang, J. Liu, P. Gong, C. Chen, B. Han, and Z. Wu, "Trajectory prediction of seagoing ships in dynamic traffic scenes via a gated spatio-temporal graph aggregation network," *Ocean Eng.*, vol. 287, Nov. 2023, Art. no. 115886.

[12] Y. Xiao, X. Li, W. Yao, J. Chen, and Y. Hu, "Bidirectional data-driven trajectory prediction for intelligent maritime traffic," *IEEE Trans. Intell. Transp. Syst.*, vol. 24, no. 2, pp. 1773–1785, Feb. 2023.

[13] Y. Liu, Z. Qin, and J. Liu, "An improved genetic algorithm for the granularity-based split vehicle routing problem with simultaneous delivery and pickup," *Mathematics*, vol. 11, no. 15, p. 3328, Jul. 2023.

[14] S. Wang, Y. Li, and H. Xing, "A novel method for ship trajectory prediction in complex scenarios based on spatio-temporal features extraction of AIS data," *Ocean Eng.*, vol. 281, Aug. 2023, Art. no. 114846.

[15] Z. Zhao, K. Ji, X. Xing, H. Zou, and S. Zhou, "Ship surveillance by integration of space-borne SAR and AIS–review of current research," *J. Navigat.*, vol. 67, no. 1, pp. 177–189, 2014.

[16] Z. Zhao, K. Ji, X. Xing, H. Zou, and S. Zhou, "Ship surveillance by integration of space-borne SAR and AIS–further research," *J. Navigat.*, vol. 67, no. 2, pp. 295–309, 2014.

[17] H. Yu, A. T. Murray, Z. Fang, J. Liu, G. Peng, M. Solgi, and W. Zhang, "Ship path optimization that accounts for geographical traffic characteristics to increase maritime port safety," *IEEE Trans. Intell. Transp. Syst.*, vol. 23, no. 6, pp. 5765–5776, Jun. 2022.

[18] S.-K. Zhang, G.-Y. Shi, Z.-J. Liu, Z.-W. Zhao, and Z.-L. Wu, "Data-driven based automatic maritime routing from massive AIS trajectories in the face of disparity," *Ocean Eng.*, vol. 155, pp. 240–250, May 2018.

[19] D. Zhang, Y. Zhang, and C. Zhang, "Data mining approach for automatic ship-route design for coastal seas using AIS trajectory clustering analysis," *Ocean Eng.*, vol. 236, Sep. 2021, Art. no. 109535.

[20] A. Nowy, K. Łazuga, L. Gucma, A. Androjna, M. Perkovič, and J. Srše, "Modeling of vessel traffic flow for waterway design–port of świnoujście case study," *Appl. Sci.*, vol. 11, no. 17, p. 8126, Sep. 2021.

[21] D. Zissis, K. Chatzikokolakis, G. Spiliopoulos, and M. Vodas, "A distributed spatial method for modeling maritime routes," *IEEE Access*, vol. 8, pp. 47556–47568, 2020.

[22] M. McBride, M. Boll, and M. Briggs, "Harbour approach channels—Design guidelines," PIANC, Gen. Secretarriat Boulevard Roi Albert II, Brussels, Belgium, PIANC Rep. 121, Jan. 2014.

[23] Z. Xiao, X. Fu, L. Zhang, and R. S. M. Goh, "Traffic pattern mining and forecasting technologies in maritime traffic service networks: A comprehensive survey," *IEEE Trans. Intell. Transp. Syst.*, vol. 21, no. 5, pp. 1796–1825, May 2020.

[24] G. Pallotta, M. Vespe, and K. Bryan, "Traffic knowledge discovery from AIS data," in *Proc. 16th Int. Conf. Inf. Fusion*, Istanbul, Turkey, Jul. 2013, pp. 1996–2003.

[25] G. Pallotta, M. Vespe, and K. Bryan, "Vessel pattern knowledge discovery from AIS data: A framework for anomaly detection and route prediction," *Entropy*, vol. 15, no. 6, pp. 2218–2245, Jun. 2013.

[26] M. Fiorini, A. Capata, and D. D. Bloisi, "AIS data visualization for maritime spatial planning (MSP)," *Int. J. e-Navigat. Maritime Economy*, vol. 5, pp. 45–60, Dec. 2016.

[27] D. Liu, H. Rong, and C. Guedes Soares, "Shipping route modelling of AIS maritime traffic data at the approach to ports," *Ocean Eng.*, vol. 289, Dec. 2023, Art. no. 115868.

[28] P. A. M. Silveira, A. P. Teixeira, and C. G. Soares, "Use of AIS data to characterise marine traffic patterns and ship collision risk off the coast of Portugal," *J. Navigat.*, vol. 66, no. 6, pp. 879–898, 2013.

[29] X. Wu, A. L. Mehta, V. A. Zaloom, and B. N. Craig, "Analysis of waterway transportation in Southeast Texas waterway based on AIS data," *Ocean Eng.*, vol. 121, pp. 196–209, Jul. 2016.

[30] M. Lloyds, "Study of maritime traffic flows in the Mediterranean Sea," in *Proc. Regional Mar. Pollut. Emerg. Response Centre Mediterr. SEA (REMPEC)*, 2008, p. 39.

[31] J.-S. Lee, H.-T. Lee, and I.-S. Cho, "Maritime traffic route detection framework based on statistical density analysis from AIS data using a clustering algorithm," *IEEE Access*, vol. 10, pp. 23355–23366, 2022.

[32] J. Yang, L. Ma, and J. Liu, "Modeling and application of ship density based on ship scale conversion and grid," *Ocean Eng.*, vol. 237, Oct. 2021, Art. no. 109557.

[33] E. Osekowska, H. Johnson, and B. Carlsson, "Grid size optimization for potential field based maritime anomaly detection," *Transp. Res. Proc.*, vol. 3, pp. 720–729, Jan. 2014.

[34] I. Kontopoulos, I. Varlamis, and K. Tserpes, "A distributed framework for extracting maritime traffic patterns," *Int. J. Geographical Inf. Sci.*, vol. 35, no. 4, pp. 767–792, 2021.

[35] K.-I. Kim, J. S. Jeong, and G.-K. Park, "Development of a gridded maritime traffic DB for e-navigation," *Int. J. e-Navigat. Maritime Economy*, vol. 1, pp. 39–47, Dec. 2014.
[36] P.-R. Lei, T.-H. Tsai, and W.-C. Peng, "Discovering maritime traffic route from AIS network," in *Proc. 18th Asia–Pacific Netw. Oper. Manage. Symp. (APNOMS)*, Oct. 2016, pp. 1–6.
[37] L. Falco, A. Pittito, W. Adnams, N. Earwaker, and H. Greidanus, "Eu vessel density map detailed method," EMODnet Hum. Activities, Roma, Italy, Tech. Rep. v 1.6, 2023. [Online]. Available: https://emodnet.ec.europa.eu/sites/emodnet.ec.europa.eu/files/public/HumanActivities_20231101_VesselDensityMethod.pdf
[38] L. Wu, Y. Xu, Q. Wang, F. Wang, and Z. Xu, "Mapping global shipping density from AIS data," *J. Navigat.*, vol. 70, no. 1, pp. 67–81, 2017.
[39] R. Manonmani, S. Prabaharan, R. Vidhya, and M. Ramalingam, "Application of GIS in urban utility mapping using image processing techniques," *Geo-spatial Inf. Sci.*, vol. 15, no. 4, pp. 271–275, 2012.
[40] M. Chau, M. Dzieszko, and R. Goralski, "The marine GIS-dynamic GIS in action," *Int. Arch. Photogramm., Remote Sens. Spatial Inf. Sci.*, vol. 35, pp. 688–693, Jan. 2004.
[41] S. Yun, D. Kim, S. Kim, D. Kim, and H. Kim, "Global path planning for autonomous ship navigation considering the practical characteristics of the Port of Ulsan," *J. Mar. Sci. Eng.*, vol. 12, no. 1, p. 160, 2024.
[42] G. Li and H. Zhang, "A Bézier curve based ship trajectory optimization for close-range maritime operations," in *Proc. Int. Conf. Offshore Mech. Arctic Eng.*, 2017, Art. no. V07BT06A026.
[43] W. Lee and S.-W. Cho, "AIS trajectories simplification algorithm considering topographic information," *Sensors*, vol. 22, no. 18, p. 7036, Sep. 2022.
[44] Z. Wei, X. Xie, and X. Zhang, "AIS trajectory simplification algorithm considering ship behaviours," *Ocean Eng.*, vol. 216, Nov. 2020, Art. no. 108086.
[45] S. Bhatia, "The power of the representativeness heuristic," in *Proc. 37th Annu. Conf. Cogn. Sci. Soc. (CogSci)*, Pasadena, CA, USA, Jul. 2015, pp. 1–6. [Online]. Available: https://www.sas.upenn.edu/~bhatiasu/Bhatia%202015%20CogSci%20PP.pdf
[46] X. Tong, W. Shi, and S. Deng, "A probability-based multi-measure feature matching method in map conflation," *Int. J. Remote Sens.*, vol. 30, no. 20, pp. 5453–5472, 2009.
[47] A. Samal, S. Seth, and K. Cueto, "A feature-based approach to conflation of geospatial sources," *Int. J. Geographical Inf. Sci.*, vol. 18, no. 5, pp. 459–489, 2004.
[48] T. Wenjing, H. Yanling, Z. Yuxin, and L. Ning, "Research on areal feature matching algorithm based on spatial similarity," in *Proc. Chin. Control Decis. Conf.*, Yantai, China, Jul. 2008, pp. 3326–3330.
[49] F. Zhonglianga and W. Jianhuaa, "Entity matching in vector spatial data," in *Proc. XXI ISPRS Congr.*, Beijing, China, 2008, pp. 1467–1472.
[50] L. Huang, S. Wang, Y. Ye, B. Wang, and L. Wu, "Feature matching in cadastral map integration with a case study of Beijing," in *Proc. 18th Int. Conf. Geoinform.*, Beijing, China, Jun. 2010, pp. 1–4.
[51] M. Žižović, B. Miljković, and D. Marinković, "Objective methods for determining criteria weight coefficients: A modification of the CRITIC method," *Decis. Making: Appl. Manag. Eng.*, vol. 3, no. 2, pp. 149–161, 2020.
[52] C. L. Hwang and A. S. M. Masud, *Multiple Objective Decision Making Methods and Applications*. Berlin, Germany: Springer, 1979.
[53] M. Zeleny, *Multiple Criteria Decision Making Kyoto 1975*. Berlin, Germany: Springer, 2012.
[54] D. Diakoulaki, G. Mavrotas, and L. Papayannakis, "Determining objective weights in multiple criteria problems: The critic method," *Comput. Oper. Res.*, vol. 22, no. 7, pp. 763–770, 1995.
[55] J. Ma, Z. Fan, and L. Huang, "A subjective and objective integrated approach to determine attribute weights," *Eur. J. Oper. Res.*, vol. 112, no. 2, pp. 397–404, 1999.
[56] A. Charnes, W. W. Cooper, and E. Rhodes, "Measuring the efficiency of decision making units," *Eur. J. Oper. Res.*, vol. 2, no. 6, pp. 429–444, 1978.
[57] A. R. Krishnan, M. M. Kasim, R. Hamid, and M. F. Ghazali, "A modified CRITIC method to estimate the objective weights of decision criteria," *Symmetry*, vol. 13, no. 6, p. 973, May 2021.
[58] J. Kim, Y. Huh, D. Kim, and K. Yu, "A new method for automatic areal feature matching based on shape similarity using CRITIC method," *J. Korean Soc. Surveying, Geodesy, Photogramm. Cartography*, vol. 29, no. 2, pp. 113–121, 2011.
[59] Y. I. Kim, D. H. Kim, and S. O. Lee, "Shape similarity analysis for verification of hazard map for storm surge: Shape criterion," *J. Korean Soc. Disaster Secur.*, vol. 12, no. 3, pp. 13–24, 2019.
[60] M. Series. (2010). *Technical Characteristics for an Automatic Identification System Using Time-Division Multiple Access in the VHF Maritime Mobile BAND*. [Online]. Available: https://www.itu.int/dms_pubrec/itur/rec/m/R-REC-M.1371-5-201402-I!!PDF-E.pdf
[61] Y.-J. Kim, J.-S. Lee, A. Pititto, L. Falco, M.-S. Lee, K.-K. Yoon, and I.-S. Cho, "Maritime traffic evaluation using spatial–temporal density analysis based on big AIS data," *Appl. Sci.*, vol. 12, no. 21, p. 11246, Nov. 2022.
[62] Ministry of Oceans and Fisheries (MOF). (2019). *Marine Spatial Characteristic Assessment*. Sejong, Republic of Korea. Accessed: Feb. 29, 2024. [Online]. Available: https://www.law.go.kr/admRulSc.do?menuId=5&subMenuId=41&tabMenuId=183&eventGubun=060115#
[63] H.-J. Kim, "A new method for calculating quantiles of grouped data based on the frequency polygon," *J. Korean Data Inf. Sci. Soc.*, vol. 28, no. 2, pp. 383–393, 2017.
[64] E. Bodansky, A. Gribov, and M. Pilouk, "Smoothing and compression of lines obtained by raster-to-vector conversion," in *Proc. Graph. Recognit. Algorithms Appl., 4th Int. Workshop (GREC Kingston)*, Ontario, ON, Canada, Sep. 2002, pp. 256–265.
[65] G. E. Farin and G. Farin Eds., *Curves and Surfaces for CAGD: A Practical Guide*. Burlington, MA, USA: Morgan & Kaufmann, 2002.
[66] D. H. Douglas and T. K. Peucker, "Algorithms for the reduction of the number of points required to represent a digitized line or its caricature," *Cartographica: Int. J. Geographic Inf. Geovis.*, vol. 10, no. 2, pp. 112–122, Dec. 1973.
[67] Z. Wang and J.-C. Müller, "Line generalization based on analysis of shape characteristics," *Cartography Geographic Inf. Syst.*, vol. 25, no. 1, pp. 3–15, Jan. 1998.
[68] P. F. Fisher, S. Zhou, and C. B. Jones, "Shape-aware line generalisation with weighted effective area," in *Proc. Develop. Spatial Data Handling: 11th Int. Symp. Spatial Data Handling*, 2005, pp. 369–380.
[69] W. Visvalingam and J. D. Whyatt, "Line generalization by repeated elimination of the smallest area," *Cartographic J.*, vol. 30, no. 1, pp. 46–51, Jun. 1993.
[70] D. Burghardt and S. Steiniger, "Usage of principal component analysis in the process of automated generalisation," in *Proc. 22nd Int. Cartographic Conf.*, 2005, pp. 9–16.
[71] Y.-M. Wang and Y. Luo, "Integration of correlations with standard deviations for determining attribute weights in multiple attribute decision making," *Math. Comput. Model.*, vol. 51, nos. 1–2, pp. 1–12, Jan. 2010.
[72] *Methodology for Assessing the Marine Navigational Safety & Emergency Response Risks of Offshore Renewable Energy Installations*, Dept. Trade Ind., New Delhi, India, 2013.

HAK-CHAN KIM received the B.S. degree from the Division of Global Maritime Studies, Korea Maritime and Ocean University (KMOU), Busan, South Korea, in 2019. He was a Lieutenant with the Republic of Korea Navy for joint military exercise. He was a Navigator of third officers with SK Shipping Company on crude oil carriers and a Korea Ship Managers' Association with Seafarer Labor·Human rights protection education as a Senior Staff. His research interests include fusion research using artificial intelligence techniques, data science, and GIS.

WOO-JU SON received the B.S. degree from the Division of Navigation Science, Korea Maritime and Ocean University (KMOU), Busan, South Korea, in 2014, the M.E. and Ph.D. degrees from the Graduate School, KMOU, in 2020 and 2023, respectively. He was a Navigation Officer and worked for heavy lift cargo carrier. He was with Maritime Traffic Safety Audit Center, KMOU, as a Researcher, and Safetech Research Company Ltd., as a Senior Level Researcher in the field of maritime traffic safety assessment. Recently, he has been a Postdoctoral Researcher with KMOU. His research focuses on utilizing data mining algorithms in maritime traffic data for safe ship operation.

JEONG-SEOK LEE received the B.S. degree from the Division of Navigation Science, Korea Maritime and Ocean University (KMOU), Busan, South Korea, in 2014, and the Ph.D. degree from KMOU, in 2023. From 2014 to 2017, he was a Navigator of the third and second officers with SK Shipping Company, gaining experience in bulk carriers, product tanker carriers, and very large crude oil carriers. In 2018, he performed related a Maritime Simulator Operator and conducted research using maritime traffic data. He is currently a Senior Researcher with Marine Big Data AI Center, Korea Institute of Ocean Science and Technology (KIOST). His research interests include utilizing marine big data, artificial intelligence, and GIS.

IK-SOON CHO received the B.Sc. degree in nautical science course, in 1996, the M.E. degree in maritime transportation science from Korea Maritime and Ocean University (KMOU), Busan, South Korea, in 2000, and the Ph.D. degree from the Graduate School of Science and Technology, Kobe University, Kobe, Japan, in 2005. He was with the Traffic Safety Audit Center, KMOU based on Korea Maritime Safety Act. He is currently a Professor with the Division of Maritime AI and Cyber Security, College of Maritime Sciences. His research interests include maritime safety evaluation, ship operating, and mooring safety analysis based on big-data using machine learning and deep learning algorithm.